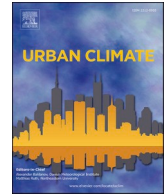




ELSEVIER

Contents lists available at [ScienceDirect](https://www.sciencedirect.com)

## Urban Climate

journal homepage: [www.elsevier.com/locate/uclim](http://www.elsevier.com/locate/uclim)

# Assessing urban heat island effects through local weather types in Lisbon's Metropolitan Area using big data from the Copernicus service

Cláudia Reis <sup>a,\*</sup>, António Lopes <sup>a,b</sup>, A. Santos Nouri <sup>c</sup>

<sup>a</sup> Universidade de Lisboa, Institute of Geography and Spatial Planning (IGOT), Centre of Geographical Studies, Rua Branca Edmée Marques, Cidade Universitária, 1600-276 Lisboa, Portugal

<sup>b</sup> Associated Laboratory Terra, Lisboa, Portugal

<sup>c</sup> Department of Interior Architecture and Environmental Design, Faculty of Art, Design and Architecture, Bilkent University, Bilkent, Turkey

## ARTICLE INFO

## Keywords:

Urban climate  
Copernicus dataset  
Local weather type  
Air temperature  
Urban heat island

## ABSTRACT

In this study UHI in Lisbon's Metropolitan Area (LMA) is analyzed through Local Weather Types (LWT) using an air temperature dataset produced by Copernicus. Over 61,000 hourly air temperature maps between 2008 and 2014 are extracted, divided into thermal seasons and LWT, and UHI is calculated by the anomaly between each raster cell and a pixel from "Low Plants" Local Climate Zone (LCZ) class. UHI daily cycle is analyzed by LWT. Statistical analysis shows that rainy days produce lower median UHI intensities (close to 0 °C), while sunny days, especially very cold winter days, produce higher UHI intensities (median values close to 1,5 °C). Analysis of the UHI pattern displays a S/SE-N/NW dichotomy in the right bank of the Tagus river and an N-S dichotomy in the Peninsula of Setúbal. The UHI effect is more pronounced in Lisbon, particularly in the riverfront area, and on the opposite bank of Tagus due to the shelter effect of frequent N winds. As previous studies have proven, UHI in LMA is mainly a nighttime phenomenon. This methodology may help decision makers to identify critical heating districts as well as weather conditions most conducive to a significant overheating of the urban atmosphere.

## 1. Introduction

Nowadays, we are experiencing critical changes in natural environments by the second. The high-speed impermeabilization and urbanization processes disturb atmospheric processes, which, subsequently, create heat "bubbles" surrounded by cooler and cleaner environments. These differences of temperature (air and surface) between an urban area and its surroundings called Urban Heat Islands (UHI) are an already well-studied phenomenon in urban climate and spatial planning literature (Arnfield, 2003; He, 2018; Oke et al., 2017). Since urban population numbers are expected to increase significantly by the middle of this century (approximately 66%, according to the United Nations, n.d., Population Division), contemporary urban decision-making face severe challenges to ensure and promote favorable encompassing human thermal comfort thresholds for urban inhabitants. Hence, the risk associated with the warming of the built environment affects both outdoor and indoor contexts, with the additional aggravator of the elderly and other

Abbreviations: UHI, Urban Heat Island; LCZ, Local Climate Zone; LWT, Local Weather Type; LMA, Lisbon Metropolitan Area.

\* Corresponding author.

E-mail address: [claudiareis2@campus.ul.pt](mailto:claudiareis2@campus.ul.pt) (C. Reis).

<https://doi.org/10.1016/j.uclim.2022.101168>

Received 9 February 2022; Received in revised form 1 April 2022; Accepted 9 April 2022

Available online 19 April 2022

2212-0955/© 2022 Published by Elsevier B.V. This is an open access article under the CC BY license (<http://creativecommons.org/licenses/by/4.0/>).

vulnerable groups which are frequently located in thermally vulnerable settlements.

Local weather conditions are one of the fundamental drivers of UHI development (Liu et al., 2020; Ngarambe et al., 2021; Yang et al., 2020). For this reason, the relation between UHI intensities/patterns and singular climate variables like wind speed/direction, cloud cover, and precipitation (although to a smaller extent), has been analyzed and quantified in previous studies (Du et al., 2016; Giannaros and Melas, 2012; He, 2018; Lauwaet et al., 2016; Lee and Baik, 2010; Morris et al., 2001). According to Oke et al. (2017), wind promotes atmospheric transport and mixing, which limits horizontal and vertical temperatures differences, while cloud cover has a strong control on shortwave and longwave radiation exchanges which are the main drivers of heating and cooling, respectively. On the other hand, humidity and pressure are less strongly correlated with UHI than wind and cloud cover (Oke et al., 2017).

Since the focus is primarily on the isolated effect of each climate variable, there is little to no information about the change of patterns when meteorological conditions are different than clear skies and weak winds. According to Yang et al., 2020, the seasonality of meteorological variables has complex effects on urban-rural thermal differences. However, if one is to consider the full range of “local weather typology”, which comprises the conditions of the atmospheric boundary layer that surrounds the city (Lopes et al., 2020), like air temperature, humidity, wind (sources, direction, and speed), precipitation and solar radiation, the combinations of all these climate variables are far too complex to be reduced to the effects of wind and cloud coverage. This explains the need to synthesize the prevailing meteorological conditions and, hence, to deepen the knowledge about the climatological science of UHI intensities and patterns.

The analysis of climate phenomena at meso (local) and micro scales requires a fine mesh of meteorological data with a high temporal resolution that is barely available due to logistical and financial constraints. For these reasons, the use of climate data modeled and compiled in large datasets is an increasingly viable and valuable option. Copernicus, the European Union Earth Observation Program coordinated and managed by the European Commission in partnership with the European Space Agency, has recently released a very complete dataset that contains air temperature, specific humidity, relative humidity, and wind speed raster

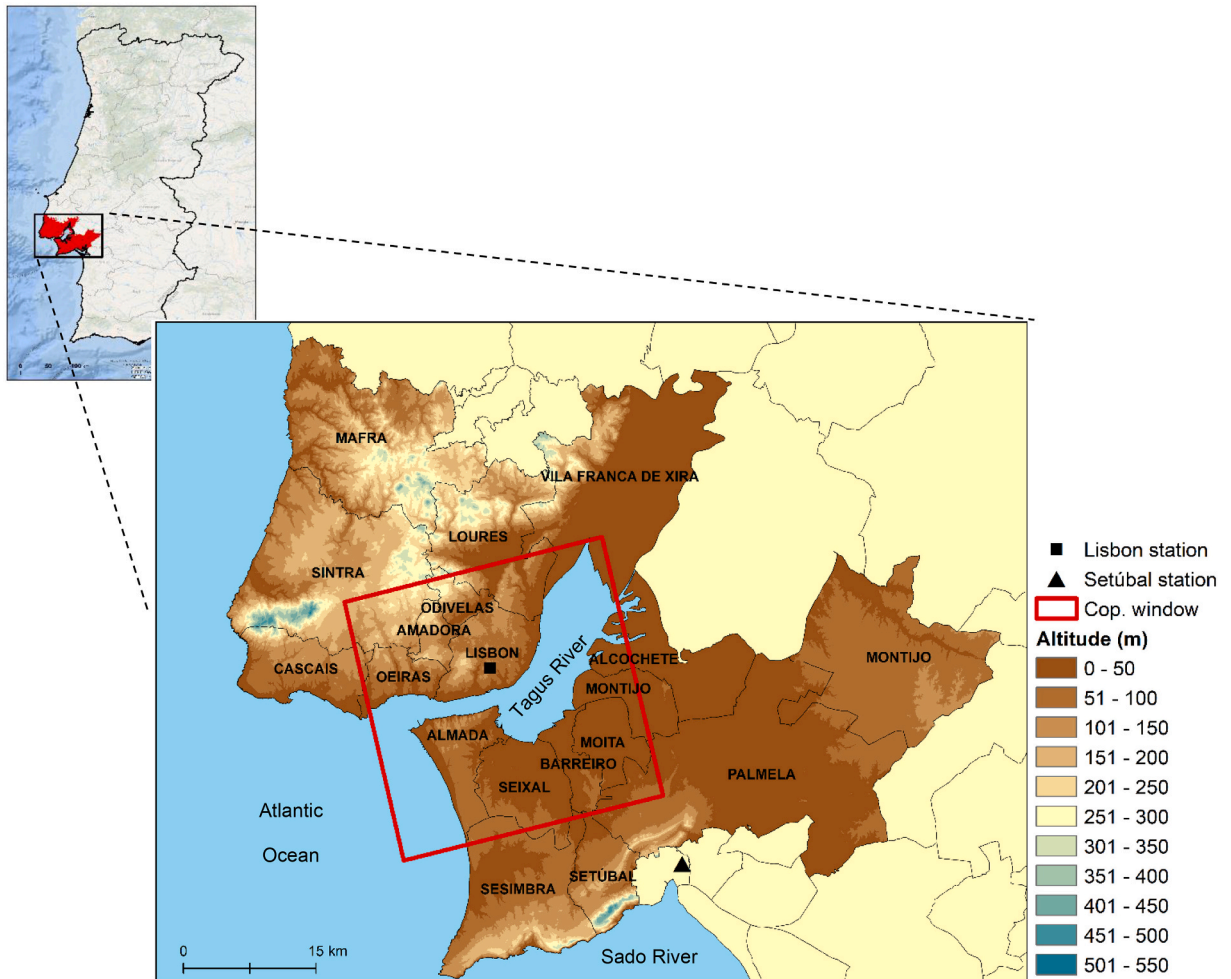


Fig. 1. Geographical position and topographic context of LMA. Source of Digital Elevation Model data: ALOS Global Digital Surface Model “ALOS World 3D - 30m (AW3D30)”, Japan Aerospace Exploration Agency (JAXA).

data for 100 European cities from 2008 to 2017. Due to its very high temporal resolution (hourly) and good spatial resolution (100\*100 m), this dataset may be quite useful for urban climate detailed analysis, especially in urban areas where field data is insufficient or inexistent.

Lisbon is a Mediterranean city in which the UHI has been subject to several investigations over the last 40 years by the Zephyrus Group (Climate Change and Environmental Systems), University of Lisbon (Alcoforado and Andrade, 2006; Alcoforado et al., 2014; Lopes et al., 2011; Lopes et al., 2013). There is already a significant amount of information regarding UHI magnitude in its daily cycle and per seasons (Lopes et al., 2013; Lopes et al., 2020; Oliveira et al., 2021). However, the possible changes considering typical meteorological conditions that characterized this city's local climate are considerably less developed. Furthermore, looking at the county limits to analyze the increase of temperature in urban areas compared to "rural"/natural spaces can be deceptive in the case of Lisbon. This is due to the intensification of regional and local urbanization processes of the adjacent territories and the massive expansion of urban fabric that took place at the beginning of the second half of the 20th century, giving rise to the constitution of Lisbon's Metropolitan Area (LMA) in the 1990s. Consequently, the increasing volume of data from remote sensing techniques and complex climate models as well as territorial geostatistical analysis and modeling techniques allow a deeper analysis of the mosaic of microclimates that comprise UHI (Lopes et al., 2020).

Thereby, the purpose of this investigation is threefold, namely:

1. to present a methodology for detailed UHI analysis by LWT that is replicable in other urban areas;
2. to analyze UHI in LMA with fine detail by Local Weather Types (LWTs) using a recent, complete, and open-source urban climate dataset and;
3. to validate UHI records generated from the Copernicus data using hourly data collected from a mesoscale meteorological network installed in Lisbon.

## 2. Materials and methods

### 2.1. Study area

The undertaken research is focused on part of the LMA, located in south-central Portugal (Fig. 1) with an area of 3015 km<sup>2</sup> and just over 2,8 million habitants, more than ¼ of the Portuguese population (2021 Census – Preliminary Results).

The respective territory incorporates 18 municipalities divided into two sub-regions (Great Lisbon, on the right bank of Tagus river, and the Peninsula of Setúbal on the left bank). Its geographic location, enclosed by the Atlantic Ocean to the west, and the Tagus and Sado rivers, and its moderate relief (Fig. 1), where altitudes reach 500 m only in Sintra (North LMA) and Arrábida (South LMA) mountains (orographic obstacles to the penetration of humid air masses – Pereira, 2003), determines a boundary position between two Mediterranean climate subtypes, 'Csa' (Mediterranean with a hot summer) and 'Csb' (Mediterranean with a cool summer), which are generally characterized by dry summers and mild and rainy winters (Peel et al., 2007).

For these reasons, both in winter and in summer seasons there is a West (W) - East (E) dichotomy in the temperature regime. The western coast of Lisbon and Setubal Peninsulas benefits from the moderating effect of the ocean, mitigating extreme heat in summer and preventing the formation of frost in winter (Lopes et al., 2018). Further inland, the valley bottoms of the North (N) LMA and the alluvial areas of the Tagus and Sado rivers are more prone to the accumulation and stagnation of cold air flows in winter since they benefit from the shelter of important regional mountains. In summer air temperatures may reach 40 °C in really hot days (Lopes et al., 2018). According to the climate normal (1971–2000, Lisbon/Geophysical – Fig. 1), the average annual daily temperature reaches 17 °C while in Setúbal drops to 16,2 °C and in both locations varies considerably throughout the year. In January, the coldest month, the air temperature is 9,9 °C in Setúbal and 11,3 °C in Lisbon, but in summer daily mean temperatures reach 23 °C in both cities (August). However, the number of hot days (maximum daily temperatures ≥30 °C) is considerably higher in Setubal (13 days and 8 days in Lisbon, in July). Furthermore, annual average precipitation surpasses 700 mm and over 75% of the rain occurs in the cooler semester (between October and March).

As for the wind regime, the topography of the LMA and the proximity to relevant water bodies as well as the urban morphology have a direct influence on the direction and speed components. At an annual scale, dominant winds come from N in N LMA and Northwest (NW) and W in South (S) LMA (Lopes et al., 2018). These N and NW winds have been partially blocked in urban areas as is the case of Lisbon by the growth of the built-up area to N, which causes serious problems for cooling the city and dispersing pollutants (Lopes et al., 2011). The city center is often cooled on 35% of summer days when the ocean and Tagus estuary breezes reach this area (Vasconcelos and Lopes, 2006). Still, in the winter season N and Northeast (NE) winds represent 27% of the occurrences, while Southwest (SW) and S winds, which are generally moister and unstable air masses, account for 29% of occurrences (Lopes, 2003).

Urban morphology and geometry alter aerodynamic conditions and radiative and energetic exchanges and, for that, influence UHI spatial distribution and magnitude (Correia, 2019; Oke et al., 2017). As for the case of Lisbon, Correia (2019) recently calculated a set of indicators that evaluate degrees of urban compactness (considering height and proximity of buildings), volumetry, and aerodynamic roughness (the friction caused by surface roughness with effects on ventilation conditions). About 69% of Lisbon's city area presents a low urban density with moderate roughness, low compactness, and low volumetric index and only 8.4% is classified as high-density areas (Correia, 2020). - However, the old city center located at the riverfront and the northern and NW areas are considered hot spots in the city with a very high volumetric index. Additionally, in the downtown area the average building height ranges between 10 and 25 m but the distance between buildings is usually low and, hence, this building height/street width (H/W) ratio is high as well as the compactness ratio. The N and NW parts of the city present the highest levels of aerodynamic roughness due to the building heights,

between 25 and 65 m, but the ratio between building height and distance is lower due to the greater width of the streets as well as the high sky view factor (SVF).

## 2.2. UHI intensity, pattern and daily cycle by LWT in LMA

The procedures to determine UHI intensity, pattern and daily cycle by LWT are synthesized in four main steps (Fig. 2).

The first step corresponds to the production of a LWT classification that incorporates an array of different climate variables integrated into the K-means cluster analysis (Section 2.2.1.). Then, hourly air temperature records for the LMA were extracted from the Copernicus dataset (Section 2.2.2.) and divided by thermal seasons and LWT and, then, UHI was calculated using an urban mask from a recently updated LCZ classification (Section 2.2.3.). In order to validate this dataset, nine measuring points from a mesoscale meteorological network (CEG-IGOT) were plotted against modeled air temperature records (Section 2.2.4.).

### 2.2.1. LWT in Lisbon

The application of LWT classifications for urban climate and, especially, UHI studies is still very recent and underestimated. Decomposing Lowry's eq. (1977), the climate of a city is the result of the sum of three components: the "background" climate, the local landscape effect and the urban effect. The LWT classification corresponds to the first component, which relates to the analysis of climate conditions without the presence of either landscape or urban effects (Lowry, 1977). According to Hidalgo and Jouglé (2018) this methodology allows to simplify the plurality of weather conditions representative of a location. The LWT classification used in this investigation was already produced for Lisbon (Reis et al., 2020). The methodology was adapted from the work of Hidalgo and Jouglé (2018) for Toulouse (France) and based on cluster analysis (k-means) using hourly data of air temperature, wind speed and direction, accumulated precipitation, cloud cover, and specific humidity registered at Lisbon's Airport Weather Station (AWS) (Portela – Fig. 3).

The data was divided into daytime, nighttime, and annual thermal regimes. These thermal seasons were generated considering the annual cycle of maximum and minimum daily air temperatures (Table 1). Further details about this classification can be found in Reis et al., 2020. First of all, the initial LWT classification, based on data from 2009 to 2018, was extended to 2004.

Since the idea was to compare UHI outputs obtained from Copernicus data (2008–2017) with field data from CEG/IGOT mesoscale meteorological network (2004–2014; Lopes et al., 2013), there was a need to match the data periods. For that, the cluster centroids from the initial classification were used to assign each respective day between 2004 and 2008 an LWT. However, given the considerable size of the LWT generated (29 LWT divided into 8 sets), it proved too large to analyze further details, and it was found that in most cases the meteorological conditions observed during the day remain with no major shifts at night.

As a result, the matching day and night LWT were grouped into daily LWT. Those correspondences were established between daytime and nighttime LWT within the same thermal season using the thresholds for each climate variable stipulated for the LWT nomination (Reis et al., 2020). The days whose daytime and nighttime weather conditions were relatively similar (same dominant wind direction and, at least, two out of five similar climate thresholds) were grouped into one LWT.

It was found a correspondence between day and night LWT in 92% of summer days (1655 in 1801), 84% of winter days (1249 in 1487), 79% of spring days (1164 in 1469), and only in 53% of fall days (373 out of 710), which shows a certain amount of unpredictability and instability of the meteorological conditions in transition seasons. The remaining days whose meteorological conditions changed rapidly from day to night were excluded from this grouping. Table 2 indicates the frequency of occurrence of each daily LWT. LWT with N and NW dominant winds are quite frequent across seasons in Lisbon, as the existing literature about this city's wind fields states. This happens especially in the summer season. In the remaining seasons, other LWT emerge with winds from the S and W quadrants, typically rainy (maritime air masses, normally more unstable, and in winter associated with the trajectory of frontal systems). Still, in winter and autumn, eastern winds (E and NE) appear more predominantly, typically drier and providing very cold weather (possible cold spells), clear skies, and absence of precipitation, which implies atmospheric stability. Furthermore, all winter LWT are generally (even the rainiest conditions) dry and all summer LWT are quite humid related with the ocean proximity. In the transition seasons, both wet and dry air masses affect meteorological conditions in Lisbon.

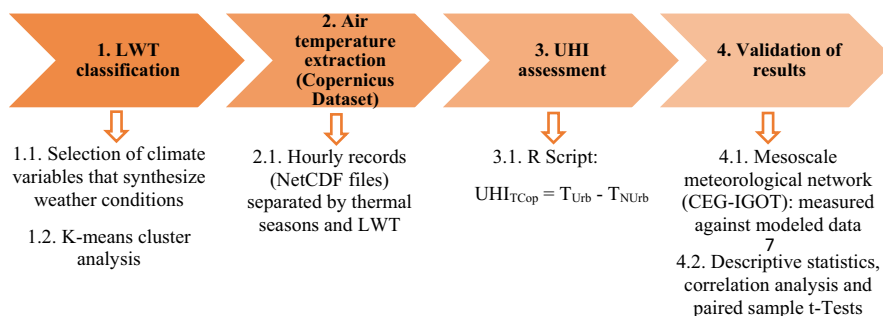
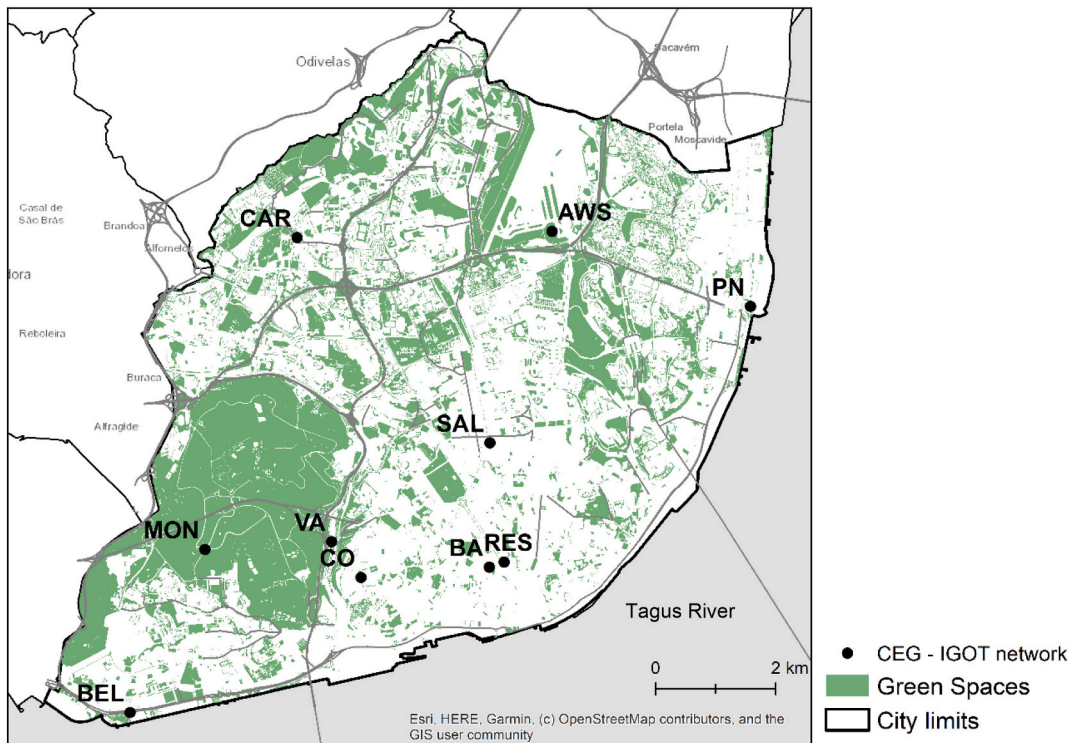


Fig. 2. UHI assessment by LWT in LMA: framework.



**Fig. 3.** CEG/IGOT mesoscale meteorological network: CAR – Carnide; MON – Monsanto; SAL – Saldanha; BEL – Belém; VA – Vale de Alcântara; CO – Campo de Ourique; RES – Restauradores; BA – Bairro Alto; PN – Parque das Nações. AWS – Lisbon's airport weather station. Source of green spaces data: Geodados, Lisbon City Hall (theme: Green Spaces). (For interpretation of the references to colour in this figure legend, the reader is referred to the web version of this article.)

**Table 1**  
Thermal seasons in Lisbon: duration and attributes. (Reis et al., 2020).

Periods	Duration	T °C		
		Minimum	Mean	Maximum
Winter	26/11 to 04/03	8,6	11,7	14,7
Spring	05/03 to 10/06	12,5	16,6	20,6
Summer	11/06 to 08/10	17,7	22,7	27,7
Autumn	09/10 to 25/11	13,4	16,8	20,2

### 2.2.2. Copernicus urban climate dataset

To produce detailed cartography about the UHI distribution in the LMA, the dataset presented by the Copernicus Climate Change Service was used in this study. This large dataset offers air temperature, specific humidity, relative humidity, and wind speed data for 100 European cities (2008–2017) with a spatial resolution of 100 m, with an hourly temporal resolution (<https://cds.climate.copernicus.eu/cdsapp#!/dataset/sis-urban-climate-cities?tab=overview>). It was generated using the urban climate model *UrbClim*. According to Hooyberghs et al., 2019; Kourtidis et al., 2015; De Ridder et al., 2015; and Zhou et al., 2016, *UrbClim* consists of a downscaling of a land surface scheme containing urban physics coupled to a 3D atmospheric boundary layer module.

In this case, two different types of data were incorporated: large-scale weather conditions (downscaling of ERA 5 reanalysis) and terrain data (Table 3).

More information about this model can be found in Hooyberghs et al., 2019. Air temperature layer represents thermal conditions at 2 m above the surface. Table 4 synthesizes this data details.

Therefore, air temperature files were extracted in NetCDF-4 format for LMA between 2008 and 2014. In total, 61,368 hourly air temperature files were extracted, 20,190 (32,9%) representing summer season, 16,814 (27,4%) for winter, 16,447 (26,8%) for spring and 7917 (12,9%) for autumn. After this procedure, all information was divided by LWT. Since the hourly maps were in UTC format, a conversion of the data to Lisbon local time was made straightforward.

### 2.2.3. UHI assessment

According to the literature, UHI intensity is measured by the difference, at a given time, between the hottest location inside an

**Table 2**  
Frequency of LWT per thermal season in Lisbon (2008–2014).

	Daily LWT designation	Frequency of days per thermal season (%)
Summer	Mild, cloudy and humid with light rain and moderate NW winds ( <b>SUmild_cloudy</b> )	14,9
	Mild, sunny and humid with moderate NW and N winds ( <b>SUmildNW</b> )	26,1
	Mild, sunny and humid with strong N winds ( <b>SUmildN</b> )	22,7
	Hot, sunny and humid with moderate N winds ( <b>SUhot</b> )	6,4
	Very hot, sunny and humid with moderate N winds ( <b>SUvhot</b> )	21,4
Winter	Cold, cloudy and dry with weak and variable winds, specially from N and NW ( <b>WcoldN</b> )	29
	Cold, cloudy, rainy and dry with moderate SW and W winds ( <b>WcoldSW</b> )	7,1
	Very cold, sunny and dry with moderate N winds ( <b>WvcoldN</b> )	26,2
	Very cold, sunny and dry with weak NE, E and N winds ( <b>WvcoldNE</b> )	21,7
	Cold, cloudy and dry with weak precipitation and moderate and variable winds, specially from NW, SW and W ( <b>ScoldNW</b> )	29,1
Spring	Cold with moderate cloud coverage, dry and with moderate N winds ( <b>ScoldN</b> )	27,9
	Mild, sunny and humid with moderate N winds ( <b>Smild</b> )	22,3
	Cold, with moderate cloud cover and dry with moderate N and NE winds ( <b>Acold</b> )	22,9
Autumn	Cool, cloudy, humid and rainy with moderate SW and W winds ( <b>Acool</b> )	9,7
	Mild, with moderate cloud cover, humid, with possibility of rain and weak N, NE and S winds ( <b>Amild</b> )	21,4

**Table 3**  
Terrain input parameters of the UrbClim model (adapted from Hooyberghs et al., 2019).

Type	Source	Resolution
Land use	Copernicus (Corine Land Cover 2012)	100 m
Soil sealing	Copernicus (Imperviousness 2012)	100 m
Vegetation index (NDV)	Copernicus (Proba V 2014–2017)	300 m
Anthropogenic heat flux	AHF 2016	0,0416 degrees
Digital Elevation Model (DEM)	U.S. Geological Survey (USGS) (Global Multiresolution Terrain Elevation Data (GMTED) 2010)	0,002083 degrees

**Table 4**  
Copernicus air temperature hourly data (Lisbon): description.

Variable	Air temperature (2 m above surface)
Unit	K
Data type	Gridded
Horizontal coverage	European
Temporal coverage	2008–2017 (extracted only 2008 to 2014)
Horizontal resolution	100 m * 100 m
Temporal resolution	Hourly
Time format	UTC
File format	NetCDF-4

urban area and a non-urban location surrounding the city/“rural” area (Martin-Vide et al., 2015; Oke et al., 2017). Alcoforado et al., 2014, give a complete dimension about this topic.

Although the Copernicus dataset covers a portion of LMA, for this calculation, only cells representing built-up areas were considered and, therefore, an urban mask was created from classes 1 to 10 of the most recent Local Climate Zones (LCZs) classification this area (Oliveira et al., 2020a, 2020b). As for the non-urban site, a cell from the LCZ D “Low Plants” class was selected as representative of the thermal behavior of these areas (Fig. 4). This cell is located at N of the airport weather station, which has been used as a reference site for almost 30 years (previous studies about Lisbon's UHI - Alcoforado, 1992; Alcoforado et al., 2014; Lopes et al., 2013), and also on the N area of Lisbon's municipality boundaries, with moderate to low urban density and a significant amount of bush and herbaceous species.

With this being said, UHI was calculated for every hour of the day between 2008 and 2014 according to the following equation:

$$UHI_{tCop} = T_{Urb} - T_{NUrb} \quad (1)$$

$UHI_{tCop}$  represents the UHI intensity of each urban cell at time t, obtained from Copernicus dataset;

$T_{Urb}$  represents air temperature of each urban cell in Copernicus grid at time t and;

$T_{NUrb}$  represents the air temperature at a non-urban site (a cell from LCZ low plants class).

For this procedure, an R (version 4.1.0.) script was constructed using the “raster” package (Hijmans and van Etten, 2012) to streamline the process given the high volume of input data. The output of this equation is a raster file with UHI intensity ( $UHI_t$ ). It should be noted that 9% of summer days, 16% of winter days, 21% of spring days, and 47% of autumn days were not used in the  $UHI_t$  estimation, since they represent days with highly variable meteorological conditions. Subsequently, all output files were classified by LWT and average  $UHI_t$  was estimated.

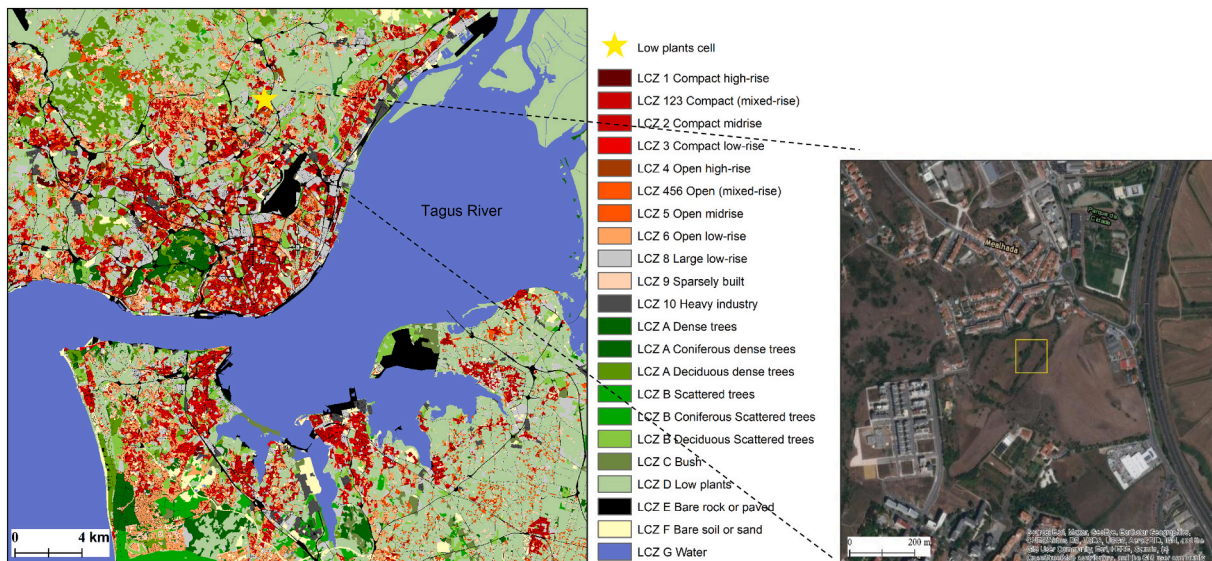


Fig. 4. LMA's updated LCZ (Oliveira et al., 2020b) and location of the non-urban site.

Later, to aggregate local weather conditions with similar  $UHI_t$ , a hierarchical cluster tree was constructed using average  $UHI_t$  records. As a clustering method, a linkage between groups was chosen and based on the squared Euclidean distance. This procedure allowed to compare spatial patterns with previous studies (Lopes et al., 2013).

#### 2.2.4. Validation of Copernicus climate data

Until now, Lisbon's  $UHI_t$  has been studied with the support of a mesoscale meteorological network (Fig. 3) operating between 2004 and 2014 carried out by CEG/IGOT - Centre of Geographical Studies—Institute of Geography and Spatial Planning of the University of Lisbon (Lopes et al., 2013). This network was composed of nine measuring points distributed by key areas registering air temperature and relative humidity every 15 min (creating average values over each hour) at 3,5 m height, inside radiation protection shields, and spaced about 1 m from the structure to avoid its thermal influence (Alcoforado et al., 2014; Lopes et al., 2013; Lopes et al., 2020; Oliveira et al., 2021). Detailed information about the geographical location, elevation and LCZ class of all nine locations can be found on Oliveira et al., 2021 (Table 1).

More concretely, two data loggers were installed on the riverfront: Belém (BEL), with low compactness and volumetric values, is located on the western part of the city and exposed to S winds and W sea breezes; on the other side, Parque das Nações (PN) is more exposed to N and E (continental) flows due to its location on the eastern riverside of the city and also with a densely populated urban environment (recent increases in building height – Lopes et al., 2020). Concerning the city center and downtown area, five data loggers were initially installed: Bairro Alto - BA (this site was not subject to analysis in the present investigation), Saldanha (SAL); Restauradores (RES even though SAL and RES are part of the most consolidated areas of Lisbon with higher compactness values, RES is slightly more sheltered from N winds and sea and estuarine breezes), Campo de Ourique (CO historic center) and Vale de Alcântara (VA as for BA, this measuring point was not investigated due to the location of the data logger, near a vegetated site). The data logger installed on Carnide (CAR) represents the northern part of the city away from the strong influence of large water bodies (the Atlantic Ocean and Tagus river) and strongly exposed to N and NW winds. Here, despite the several unbuilt interstitial areas which translate into moderate compactness levels, the building heights promote a higher aerodynamical roughness and a higher H/W ratio. Still, the data logger located on Monsanto forest hill intended to represent the thermal behavior of vegetation outside urban areas, particularly tree-type (forest) spaces (Alcoforado et al., 2014; Lopes et al., 2020). More information about this meteorological network can be found on Alcoforado et al., 2014; Lopes et al., 2013, 2020; and Oliveira et al., 2021.

Hence, the credibility of modeled air temperature in LMA from the Copernicus dataset was assessed against CEG-IGOT mesoscale network. For consistency purposes, and due to significant data gaps in all seven measuring sites, only a sample of 11,726 hourly records (end of July to December 2012; January and December 2013; January to May and August to December 2014) with no missing measurements was used for the validation procedure. In the same data period, air temperature data from the Copernicus was extracted for all seven measuring points using a GIS system and some descriptive statistics (mean, median, standard deviation, variance, percentiles) were calculated. Furthermore, several scatter plots were constructed and correlations between variables were calculated to identify a relationship between pairs of air temperature series. Additionally, paired-sample *t*-Tests were performed. This parametric test compares the means of two measurements related to the same individual, object, or unit (in this case the same location).

### 3. Results and discussion

#### 3.1. Validation of Copernicus air temperature dataset

In this section, the statistical analysis of the air temperature dataset from the Copernicus Climate Change Service is discussed. Tables 5 and 6 present a summary of some statistical measurements that allow to cross and compare measured and modeled air temperature from the seven pre-selected locations in Lisbon. According to model data, the average air temperature is consistently higher in all measuring points (between 0,3 °C and 0,5 °C) except for RES and SAL (city center). The same happens with median values, even though only in SAL median modeled air temperature matches exactly median measured values. Consecutively, modeled values reveal smaller Standard Deviations (SD) and smaller variances in all seven locations. As for variance, differences reach 3 °C in the east riverfront area of Lisbon (PN). Still, air temperature thresholds for 10th and 25th percentiles are slightly lower according to modeled and the opposite happens for the 90th percentile (except in BEL).

Fig. 5 shows the scatter plots recorded against modeled air temperature in seven measuring locations from the CEG-IGOT mesoscale meteorological network as well as correlation (r) and determination (r<sup>2</sup>) coefficients for all pairs of data. Correlation values between the seven pairs of hourly air temperature records (modeled vs measured) are positive and very strong, always above 0,9, especially in SAL, CO, and MON (r = 0,96, p. <0,05).

The results of paired-samples t-Tests for all measuring points are displayed in Table 7. Results from these t-Tests are statistically significant for a p-value of 0,05. It is possible to verify that the average differences between the seven pairs of variables (measured against modeled air temperature) are negative (except for SAL), which indicates that modeled air temperature is slightly higher in all locations. This overestimation of modeled data is more evident in the riverfront area (BEL and PN) and almost inexistent in the city center (SAL and RES), where more compact neighborhoods are dominant.

#### 3.2. UHI intensity and pattern by LWT

Fig. 6 illustrates UHI variability throughout LMA by LWT and thermal seasons.

As it can be seen, median UHI<sub>t</sub> (considering daily data) in LMA varies between 0,3 °C and 1,1 °C. Lower UHI<sub>t</sub> (close to 0 °C), as well as smaller ranges of variation (smaller interquartile ranges, about 0,6 °C; only in 5% of days median UHI<sub>t</sub> reaches 1 °C), are registered in rainy LWT, with the presence of very humid air masses coming from SW and S (WcoldSW- winter cold days with high cloud coverage and rainy with moderate daily average wind speeds of 6,5 m/s; Acool - cool autumn days with also a very high cloud cover, rainy and with average daily wind speeds around 5 m/s; SUMild\_cloudy - mild summer cloudy days with the possibility of precipitation as well as moderate winds of 5 m/s). These meteorological conditions appear on a handful of days (7% in winter, 10% in autumn, and 15% in summer). In contrast, LWT characterized by generally clear skies or with few clouds (up to 3 tenths) and, therefore, strong direct solar radiation during the day and many radiation losses to the atmosphere during the night, as is the case of very cold winter days with winds from the eastern quadrant (WvcoldNE) as well as very hot summer days (SUvhot), record higher average daily UHI<sub>t</sub> (between 1 °C and 1,4 °C) and greater ranges of variation (interquartile ranges close to 1 °C), due to greater temperature differences between day and nighttime periods. Furthermore, in 10% of these days, UHI<sub>t</sub> surpasses 2 °C. In the remaining meteorological conditions, median UHI<sub>t</sub> varies between 0,5 °C and 1 °C.

These results show a different reality from previous studies about Lisbon's UHI<sub>t</sub>. Lopes et al., 2013, found strong UHI<sub>t</sub> (>4 °C) and a higher seasonal difference mean (2,1 °C) recurrent in summer, but recorded a lower UHI<sub>t</sub> mean in winter (1,7 °C), even though the authors used the traditional astronomical seasons, which are significantly different from the thermal divisions created for this study. For instance, the coldest period of the year starts about 1 month before the astronomical winter and its end is anticipated in about 2 weeks. Furthermore, the authors did not distinguish different seasonal meteorological conditions. More specifically, and considering the example of winter UHI<sub>t</sub>, average intensities of 1,7 °C mask the inherent effect of wind direction, cloud cover, and precipitation, which are the singular climatic variables that seem to have more influence on the development and magnitude of thermal differences between the urban fabric and the adjacent "rural"/natural areas in Lisbon. Still, the authors only analyzed nine different locations while the results presented in this research surpass the city's county area and represent an array of LCZ with slightly different climatic

**Table 5**  
Measured (CEG-IGOT mesoscale meteorological network) vs Modeled (Copernicus dataset – Cop.) air temperature (°C) downtown and on the riverfront of Lisbon: Descriptive statistics.

	SAL			RES			BEL			PN			
	CEG	Cop.	Δ Cop-CEG	CEG	Cop.	Δ Cop-CEG	CEG	Cop.	Δ Cop-CEG	CEG	Cop.	Δ Cop-CEG	
Mean	16,8	16,8	0	17,2	17,2	0,0	16,7	17,2	0,5	16,8	17,2	0,4	
Median	15,7	15,7	0	16,2	16,1	-0,1	15,9	16,1	0,2	15,8	16,1	0,3	
Std. deviation (SD)	5,2	4,9	-0,3	5,1	4,9	-0,2	4,8	4,9	0,1	5,3	4,9	-0,4	
Variance	26,5	24,4	-1,1	26,2	23,9	-2,3	22,8	24,0	1,2	28,3	24,2	-4,1	
Range	31,6	28,9	-1,7	30,0	28,8	-1,2	29,0	29,0	0,0	31,6	28,7	-3,1	
Percentiles	10	10,9	11,1	0,2	11,1	11,5	0,4	10,9	11,4	0,5	10,5	11,5	1,0
	25	12,9	13,1	0,2	13,3	13,5	0,2	13,1	13,5	0,4	12,7	13,5	0,8
	75	20,5	20,2	-0,3	20,9	20,6	-0,3	20,3	20,5	0,2	20,5	20,6	0,1
	90	24,0	23,6	-0,4	24,3	24,0	-0,3	23,2	23,9	0,7	24,3	24,0	-0,3



**Table 6**

Measured (CEG-IGOT mesoscale meteorological network) vs Modeled (Copernicus dataset – Cop.) air temperature data (°C) in Monsanto, Carnide and Campo de Ourique - Descriptive statistics.

	CEG	Cop.	Δ Cop-CEG	CEG	Cop.	Δ Cop-CEG	CEG	Cop.	Δ Cop-CEG	
Mean	15,6	15,9	0,3	16,1	16,5	0,4	16,5	16,8	0,3	
Median	14,6	15,0	0,4	15,2	15,5	0,3	15,4	15,7	0,3	
Std. deviation (SD)	5,2	5,1	-0,1	5,3	5,0	-0,3	5,1	5,0	-0,1	
Variance	27,0	26,1	-0,9	27,7	25,1	-2,6	26,4	24,8	-1,6	
Range	29,7	30,4	0,7	30,4	29,1	-1,3	30,0	29,2	-0,8	
	10	9,5	9,9	0,4	9,9	10,6	0,7	10,4	10,9	0,5
Percentiles	25	11,7	12,1	0,4	12,2	12,7	0,5	12,6	13,1	0,5
	75	19,3	19,3	0,0	19,9	19,9	0,0	20,2	20,1	-0,1
	90	23,1	23,0	-0,1	23,5	23,3	-0,2	23,8	23,7	-0,1

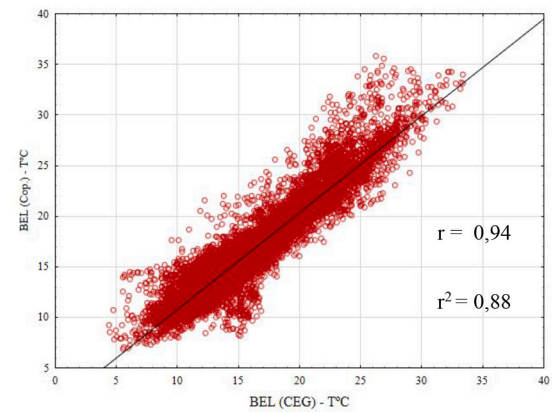
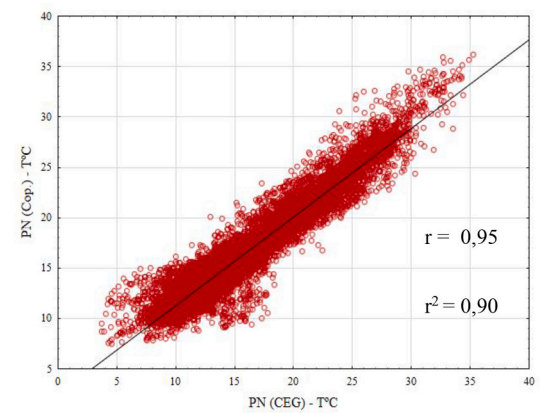
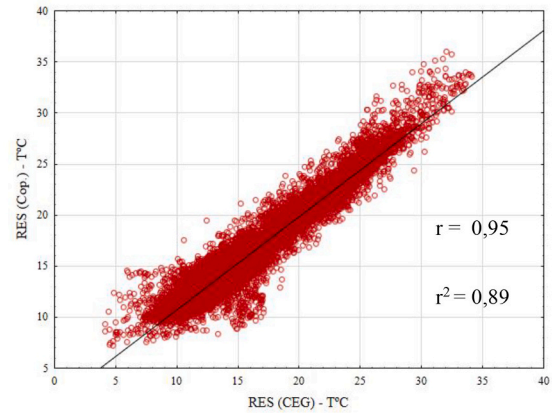
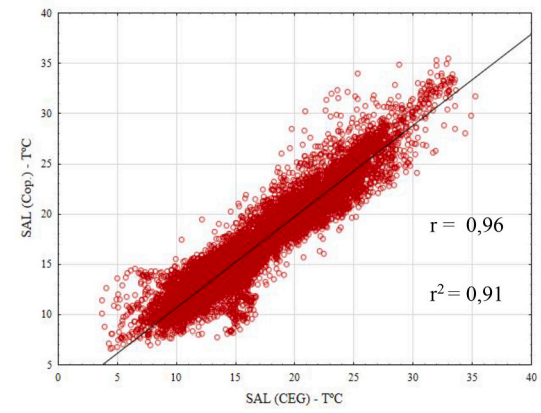
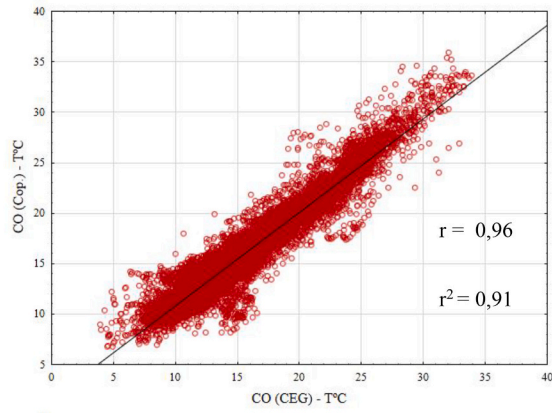
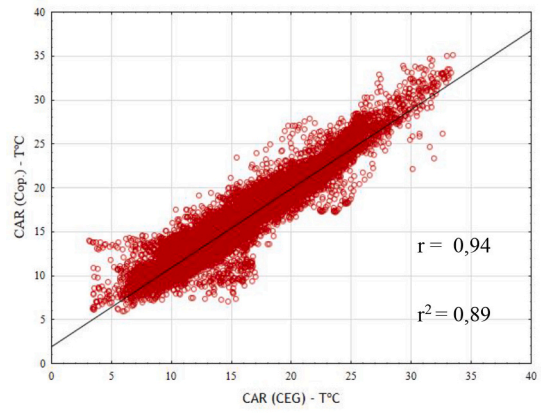
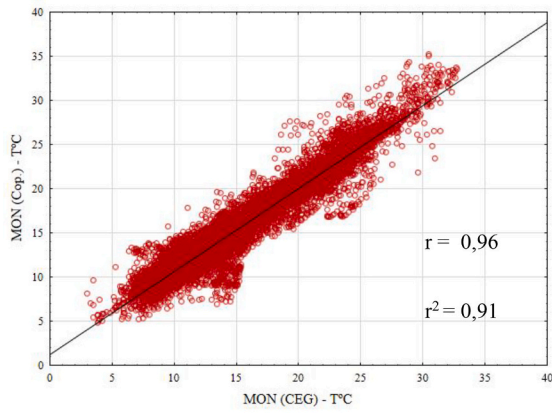
responses due to its unique land uses, even though all of them are considered as urban territory. On the other side, Copernicus air temperature maps were calculated using *UrbClim*, an urban climate model created to study  $UHI_t$  with a fine spatial resolution (a few hundred meters) whose input data is described briefly in Section 2.2.2. Even though *UrbClim* incorporates a digital elevation model, this information might not be enough to accurately generate the distribution of air temperature in LMA. This can be explained by the fact that, according to Oliveira et al., 2021, recent detailed analysis about Lisbon's daily cycle of Urban Thermal Signal (UTS) in the summer season (heatwave and non-heat wave conditions), the existence of this pattern depends mostly on prevailing wind direction. Hence, not only urban morphology but also natural topography plays a significant role in  $UHI_t$ , especially in the city center. With this being said, the lack of a topographic index capable of representing relief forms in *UrbClim* might negatively disturb the modeling of air temperature in this urban context.

Fig. 7 presents a hierarchical cluster tree of  $UHI_t$  by LWT in LMA. At a first glance, it is possible to identify five groups of LWT conditions that affect  $UHI_t$  in LMA. From left to right, the first group incorporates rainy winter and autumn LWT and summer days with high cloud cover, in which  $UHI_t$  is considerably lower. The second group distinguishes very hot summer days and spring mild days which promote stronger  $UHI_t$  (median values surpass 1 °C). The middle group incorporates an array of weather conditions, especially from summer but also from transition seasons, with low to medium-high cloud coverage, in which median  $UHI_t$  stays between 0,5 °C and 1 °C. These are followed by the group of cold/very cold winter and autumn days with weak to moderate N winds and a median  $UHI_t$  that slightly surpasses 1 °C. Finally, very cold winter days com NE and E winds are identified on their own due to the highest  $UHI_t$  in LMA. These aggregations of LWT were used for the analysis of the  $UHI_t$  daily cycle present in Section 3.3.

Fig. 8 depicts the spatial pattern of  $UHI_t$  in distinct meteorological conditions.

Despite the considerable differences in magnitude observed on both banks of the Tagus river, the UHI pattern remains relatively unchanged in all LWT, that is, recurrent hot and cool spots can be identified. Starting on the N bank of the Tagus, a S/SE – N/NW dichotomy can be observed, wherein the riverfront and the downtown area of Lisbon's municipality  $UHI_t$  is higher (between 2,5 °C and 3 °C in very cold winter days with NE and E winds but only between 1 °C and 1,5 °C in rainy winter days). This happens because of the shelter effect from the prevailing N and NW winds in Lisbon throughout the year. The city's recent growth towards the northern districts will aggravate this pattern due to the reduction in average wind speed (Lopes et al., 2011). Furthermore, the downtown area, as well as the urban fringe along the Tagus River, are already fully consolidated and with a very high soil sealing rate (little space dedicated to the vegetation). Recently, it was verified exactly that the downtown area and the continuous strip between Alcântara and PN represent the hottest places in Lisbon, with  $UHI_t$  above 4 °C (Lopes et al., 2020). Near Tagus River, generally, the E area (including PN) is slightly hotter than the W area, closer to the Atlantic Ocean (in which BEL is included). This happens because, according to Lopes et al., 2013, despite the riverbank area being affected by the estuarine breezes in the morning, it is not as exposed to the ocean as the area of BEL, which is the first site the cool sea air reaches. Also, PN cools down by regional wind flows coming from NE, which are of rare occurrence in Lisbon, or by SE breezes (Alcoforado, 1987; Vasconcelos and Lopes, 2006). Heat progresses into the main valleys, particularly Vale de Alcântara and the downtown area (BA and RES). This pattern has been known for almost 20 years, when Andrade, 2003, studied  $UHI_t$  in Lisbon and its relationship with regional atmospheric conditions, and it is the most frequent thermal mosaic in Lisbon since it appears on almost all weather conditions. Traditionally, it has been called a tentacular pattern that develops along the main axes of the development of the city (Lopes et al., 2020). As reported by Alcoforado et al., 2009, in days with weak regional winds, the core of UHI moves to the N and the downtown area remains relatively cooler due to sea/estuarine breeze situations (occur in 30% of summer days according to Lopes et al., 2013, bringing fresher air to the riverfront area of Lisbon (Alcoforado et al., 2014). Nevertheless, in the present investigation, this pattern was not found in any LWT. This might happen since the *UrbClim* model only incorporates the speed component of wind in its calculations (Hooberghs et al., 2019; Kourtidis et al., 2015; De Ridder et al., 2015; Zhou et al., 2016) and, hence, cannot model the presence of regional breezes.

$UHI_t$  decreases to NW towards sub-urban areas on the outskirts of the municipality of Lisbon (Amadora and Odivelas). On the right bank of Tagus, the most consolidated and densely built urban areas near the estuary (Almada, Seixal, Barreiro, and Moita) register  $UHI_t$  as high as on the riverfront of Lisbon. In fact, on this bank, the area in which  $UHI_t$  reaches its maximum (between 2,5 °C and 3 °C on very cold winter days, for instance) is larger than on the N bank of the LMA.



(caption on next page)

Fig. 5. Scatter plots of measured (CEG) vs modeled (Cop.) air temperature distribution in seven measuring points from CEG-IGOT meteorological network.

Table 7

Paired samples t-Test in seven measuring points from CEG-IGOT meteorological network: results.

	Paired differences				t	Sig. (2-tailed)	
	Mean	SD	Std. error mean	95% confidence interval of the difference			
				Lower			Upper
BEL: CEG / Cop.	-0,4	1,7	0,0	-0,5	-0,4	-27,2	0,00
CO: CEG / Cop.	-0,3	1,5	0,0	-0,3	-0,3	-22,3	0,00
CAR: CEG / Cop.	-0,3	1,7	0,0	-0,4	-0,3	-20,3	0,00
MON: CEG / Cop.	-0,3	1,5	0,0	-0,3	-0,3	-20,1	0,00
PN: CEG / Cop.	-0,4	1,7	0,0	-0,5	-0,4	-27,8	0,00
RES: CEG / Cop.	-0,1	1,5	0,0	-0,1	-0,1	-6,0	0,00
SAL: CEG / Cop.	0,0	1,7	0,0	-0,1	0,0	-2,3	0,02

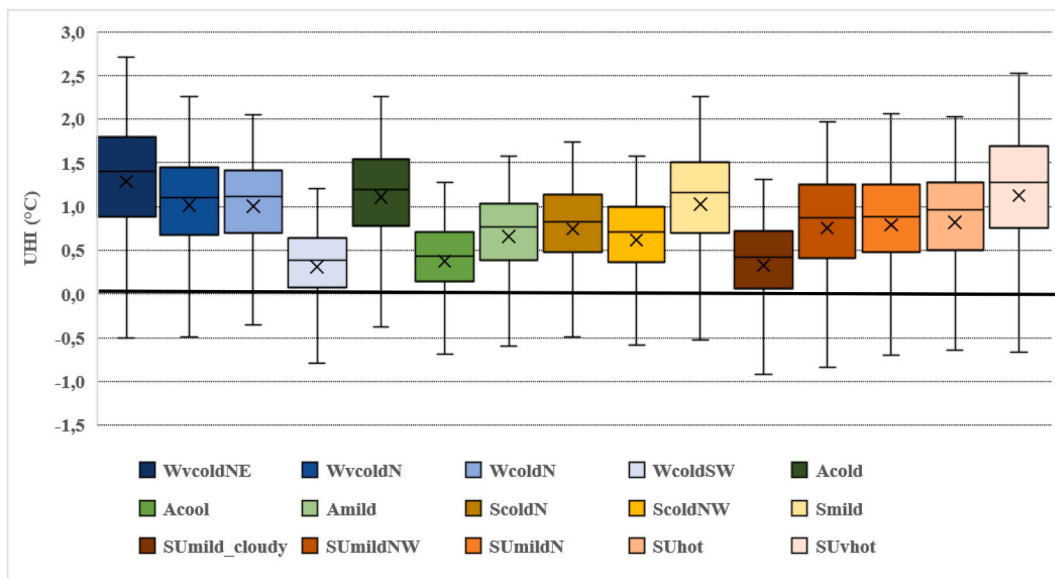


Fig. 6. LMA UHI<sub>t</sub> by LWT using hourly air temperature data from Copernicus Climate Change Service (see Table 2).

This pattern corroborates the strong influence of the variable wind on UHI<sub>t</sub> as pointed out by Alcoforado and Andrade (2006) and Oliveira et al., 2021, since the hot spots in LMA, in addition to being the most densely built urban areas (high rates of compactness and volumetry – H/W ratio close to 1), are also topographically sheltered from the dominant N winds that reach Portugal and the LMA in most of the year.

### 3.3. UHI<sub>t</sub> daily cycle by LWT

In Section 3.2. LMA UHI magnitude and pattern by LWT were presented and discussed. Since the 24 h average values previously presented mask the significant hourly changes of UHI<sub>t</sub> and, according to Oliveira et al., 2021, there is a distinct daily cycle in Lisbon, in the present investigation hourly UHI<sub>t</sub> by LWT was also analyzed in further detail. Fig. 9 presents the UHI<sub>t</sub> daily cycle in LMA.

The 6 stages were identified according to Oliveira et al., 2021, findings for the summer heatwave and non-heat wave conditions. One of the important additions to the study performed by Oliveira et al., 2021, corresponds to the decomposition of the UHI<sub>t</sub> daily cycle by the multitude of meteorological conditions that characterize Lisbon's climate. In a first instance, it is possible to observe that there are, in fact, day and nighttime divergences in UHI<sub>t</sub> and that these vary according to LWT. Mostly, rainy days are contrasted with very cold and sunny winter days and sunny spring (mild) and summer (very hot) days. In the former, the variation of UHI<sub>t</sub> throughout the day (24 h) is much smaller, as the weak interquartile range of the daily average UHI<sub>t</sub> revealed previously. During the night UHI<sub>t</sub> is positive and stable, but weak (about 0,8 °C) and during the day very weak UCI forms between 11 am and 3 pm, with UHI<sub>t</sub> rising again

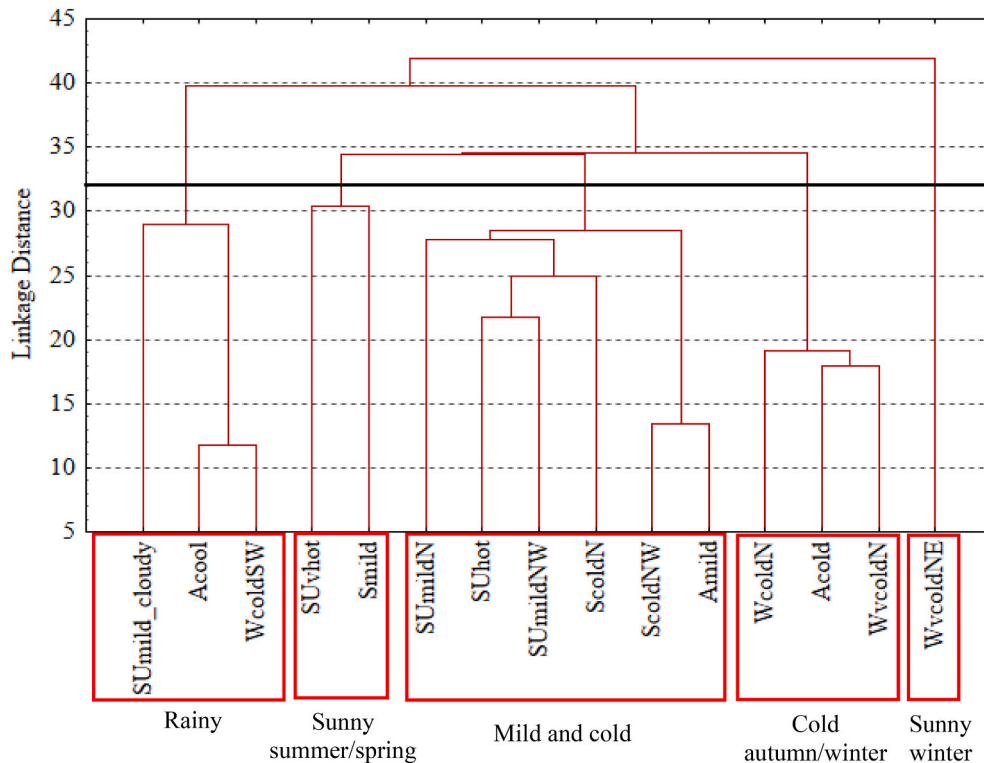


**Fig. 7.** Hierarchical cluster tree of  $UHI_t$  by LWT in LMA (see Table 2). Median  $UHI$  values:  $SU_{mild\_cloudy}$  – 0,4 °C;  $A_{cool}$  – 0,4 °C;  $W_{coldSW}$  – 0,4 °C;  $SU_{vhot}$  – 1,3 °C;  $S_{mild}$  – 1,2 °C;  $SU_{mildN}$  – 0,9 °C;  $SU_{hot}$  – 1,0 °C;  $SU_{mildNW}$  – 0,9 °C;  $ScoldN$  – 0,8 °C;  $ScoldNW$  – 0,7 °C;  $A_{mild}$  – 0,8 °C;  $W_{coldN}$  – 1,1 °C;  $A_{colod}$  – 1,2 °C;  $W_{vcoldN}$  – 1,1 °C;  $W_{vcoldNE}$  – 1,4 °C.

from late afternoon/early evening. In contrast, on very cold and sunny winter days and sunny spring and summer conditions  $UHI_t$  is relatively high and once again stable at night, approaching 2 °C, and during the day it drops again, but this time abruptly, without the formation of a UCI common on rainy days. Finally, in the late afternoon,  $UHI_t$  rises again abruptly. In the remaining sets of LWT that occur in all seasons of the year (cold autumn/winter and mild and cold), the daily path of  $UHI_t$  is closer to that of sunny winter conditions than on rainy days. In this later set of LWT, cloud cover is generally low to moderate, so day/night thermal differences are intensified, favoring the greater amplitude of daily variation of  $UHI_t$ .

The 6 stages of the  $UHI_t$  daily cycle identified by Oliveira et al., 2021, only for Lisbon city limits are also observed in all meteorological conditions. Stage 1, which corresponds to nocturnal stable  $UHI_t$ , that lasts from the late evening hours until dawn, is observed in all LWT. This stage lasts about one hour longer on sunny winter days and cold autumn and winter days (up to at 7 am) than on other weather conditions due to late sunrise, especially in the winter months (N Hemisphere). In contrast, on sunny spring and summer days when sunrise occurs earlier and from 5 am there is an immediate change in stage/beginning of the abrupt decrease in  $UHI_t$ . Stage 2 is one of transition to a UCI and Oliveira et al., 2021 observed a decrease of more than  $-0,2$  °C/h, while in this study a more accentuated decrease of  $UHI_t$  is observed in a few hours ( $-0,5$  °C). At the same time, it appears that the decrease in  $UHI_t$  is less abrupt on rainy days than in the other LWT sets. After this stage, the minimum daily peak  $UHI_t$  are observed (stage 3 – between 10 am and 11 am in all LWT, except on rainy days), which, in the case of Oliveira et al. 2021, translates into a UCI of close to  $-1$  °C, while in this study only on rainy days there is a very slight UCI ( $-0,1$  °C; on 10% of days the average  $UHI_t$  drops to  $-0,9$  °C or below, between 2 pm and 3 pm) during some hours of the day (between 11 am and 3 pm). Furthermore, on mild and cold days there is an UCI of the same intensity but only at 10 am. From 1 pm forth,  $UHI_t$  increases strongly (stage 4), a transition period that is not as abrupt as the transition period in stage 2.  $UHI_t$  reaches its maximum peak in stage 5, in late afternoon/early evening, and on very cold and sunny winter days the maximum  $UHI_t$  of 2,2 °C (in 10% of days average  $UHI_t$  surpasses 3 °C, at 8 pm) is reached 2 h earlier than in other LWT. According to Oliveira et al., 2021, this daily peak occurs earlier, around 7/8 pm. Finally, there is a transition period (stage 6) that culminates in the stabilization of  $UHI_t$  during the night (stage 1 – restart of the cycle).

Likewise, a study on the effects of heatwaves in the Lisbon county area promoted by the City Council, concerning future climate projections, found an increase in  $UHI_t$  in the early evening/late afternoon, when higher air temperatures occur (Lopes et al., 2020). With the exacerbation of maximum  $UHI_t$ , there is a greater temperature gradient between UCI (mostly from green spaces) and warmer city cores (areas with high urban density). Still, Nogueira et al., 2020, recently carried out a set of climate simulations comparing CORDEX-SURFEX-TEB models with EURO-CORDEX in Lisbon and characterized the UHI effect as well as its seasonal variations, also verifying the presence of this daily cycle with maximum positive nocturnal peaks (in the order of 4 °C) and minimum diurnal peaks

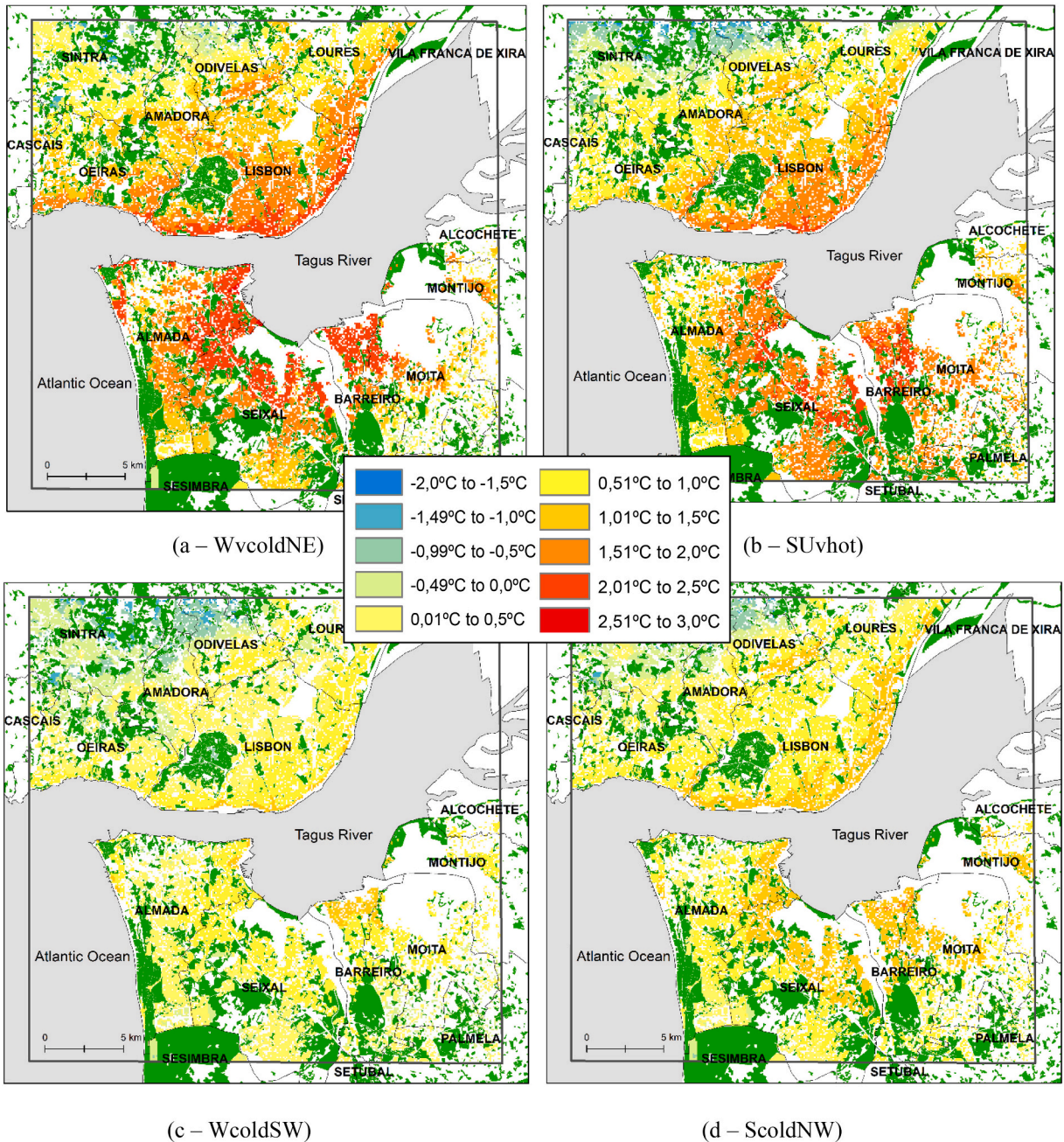


**Fig. 8.** LMA  $UHI_t$  in urban areas (other types are excluded) on (a) very cold winter days with NE and E winds (WvcoldNE); (b) Very hot, sunny, and humid summer days with moderate N winds (SUvhot); (c) Cold, cloudy, and rainy winter days with moderate SW and W winds and; (d) Cold, cloudy and dry spring days with weak precipitation and moderate and variable winds (especially from NW, SW, and W). Green spaces area represented in dark green. Non-urban areas are represented in white. (For interpretation of the references to colour in this figure legend, the reader is referred to the web version of this article.)

frequently negative (UCI), reaching intensities below  $-1\text{ }^\circ\text{C}$  in summer.

Despite the  $UHI_t$  differences between local meteorological conditions, hourly fluctuations are in agreement with international literature. According to Oke et al., 2017, canopy layer  $UHI$  is primarily a nocturnal phenomenon created because urban areas fail to cool as rapidly as the rural surroundings in the late afternoon and evening. Hence, it is driven by differences in rates of urban warming and cooling, which create the daily variation of  $UHI_t$  (Oke et al., 2017).

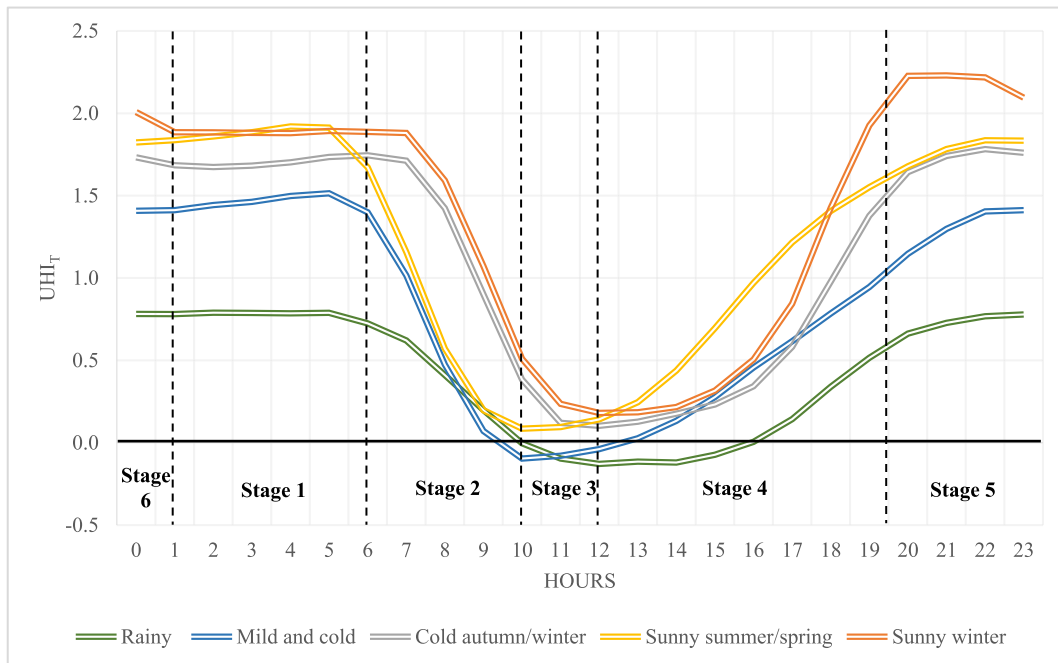


**Fig. 9.** UHI<sub>t</sub> daily cycle by LWT in LMA (3 h moving average). LWT aggregations refer to the hierarchical cluster tree in Fig. 7. Stages of the UHI<sub>t</sub> daily cycle were identified according to Oliveira et al., 2021.

#### 4. Conclusions

In the present study, UHI is analyzed by LWT in the LMA (Portugal) using a new, very complete, and freely available urban climate dataset from Copernicus Climate Change Service. Results are validated with a mesoscale meteorological network installed in Lisbon with nine measuring locations, which operated between 2004 and 2014. Main conclusions indicate:

- Very strong and positive correlations (above  $r = 0,9$ ) between measured and modeled air temperature data are registered in every location from the CEG-IGOT network. Although modeled air temperature reveals a slight overestimation of real values, especially on the riverfront area of Lisbon, the Copernicus climate variables database for numerous European cities is considered to be a reliable instrument for the study of urban climates to limit undesirable consequences of urban expansion;
- Concerning the influence of meteorological conditions on UHI<sub>t</sub> and pattern, rainy conditions with S and SW winds promote smaller thermal differences, while days with clear skies, especially in winter (very cold days with winds from the NE and E quadrant) record higher average UHI<sub>t</sub> (close to 1,5 °C);
- Precipitation (occurrence), cloud cover, and wind are confirmed as the most important climate variables in UHI development;
- As for the UHI pattern in LMA, for the diversity of weather conditions a S/SE-N/NW dichotomy on the right bank of Tagus river as well as an N-S dichotomy on the Setúbal Peninsula are identified, where the Lisbon's city limits and especially the riverfront area along with the territories near the Tagus estuary on the opposite bank (Almada, Seixal, Barreiro and Moita) correspond to recurrent hot spots due to the shelter effect from dominant N and NW winds. These excessive heating of areas with high urban density pose increased pressure on land use planning policies, which will have to prepare for realistic scenarios of rising air temperatures throughout the 21st century;
- The decomposition of the UHI daily cycle by LWT corroborates the effect of weather conditions on UHI<sub>t</sub> as well. As previous studies have shown, UHI in LMA is a nighttime thermal pattern. However, the transition stages between diurnal and nocturnal phases vary according to LWT, being smoother on rainy days and more abrupt on days with low cloud cover, as do the differences in intensity between day and nighttime periods (0,9 °C on rainy days versus 2 °C on very days winter cold with clear skies). Furthermore, only in rainy conditions is it possible to verify the formation of a very slight UCI between the late morning and early afternoon ( $-0,1$  °C, on average);

Additionally, it is important to highlight several limitations about the present investigation and the Copernicus dataset:

- Firstly, the spatial resolution of this modeled data (100 m) may be too coarse to proceed with a detailed analysis of some critical urban canyons to develop appropriate measures for improvement of human thermal comfort conditions;
- The urban climate model UrbClim used as the basis for this dataset only incorporates generic parametrization schemes and do not accommodate the topographic and climate features of the study area;

- As for the UHI calculation, due to time constraints, only one cell from the “Low Plants” LCZ class is utilized as a non-urban site, instead of a sample of cells that are representative of this class thermal behavior;
- Furthermore, the operation period of the CEG/IGOT meteorological network is not coincident with this Copernicus urban climate dataset and there are significant air temperature measurement gaps that limited the number of hourly records that are utilized for the validation procedures;
- Finally, the large amount of raster data analyzed can be quite overwhelming and time space-consuming.

Nevertheless, the present work corroborates the results of previous studies about UHI in Lisbon and extends the study area to the outskirts of this city where urbanization processes have been intensified over the last decades. This shows that not only the built environment Lisbon is warming considerably but also the densely built areas on the opposite bank of Tagus (Almada, Seixal, Barreiro, and Moita). These facts are especially concerning since these municipalities accommodate almost 1 million citizens, Lisbon alone over 500,000 habitants, and elderly people represent over 20% of inhabitants. Hence, there is a need for urban planning and design measures that limit this warming and, subsequently, thermal discomfort conditions, which are under investigation.

The methodology for estimating UHI by LWT with modeled data can be easily replicated in other urban areas where the quantity and/or quality of climate records do not provide relevant information for the development of adequate spatial planning procedures. Such a methodology conducted in this study moreover reveals and maps imperative potential intervention areas where micro/local thermal sensitive design and decision making taken by urban planners/designers, architects, and landscape architects who are equally tasked with addressing questions such as: Where are the recurrent the critical areas (hot spots) in the city? How much do these hot spots heat? When/in which weather conditions can we expect them to heat up?

Future work about this topic implies the analysis of the statistical significance of the differences between  $UHI_t$  among LWT, as well as the causes of the different behavior of  $UHI_t$  in all phases of its daily cycle according to weather conditions.

## Funding

This research was funded by FCT (Fundação para a Ciência e Tecnologia), grant number SFRH/BD/146757/2019 and the ZEPHYRUS research group of the CEG/IGOT—Universidade de Lisboa (UIDB/00295/2020 and UIDP/00295/2020).

## Declaration of Competing Interest

The authors declare that they have no known competing financial interests or personal relationships that could have appeared to influence the work reported in this paper.

## References

- Alcoforado, M.J., 1987. Brisas estivais do Tejo e do Oceano na região de Lisboa. *Finisterra* 22 (43). <https://doi.org/10.18055/Finis2013>.
- Alcoforado, M.J., 1992. O clima da região de Lisboa. *Contrastes e ritmos térmicos. Memórias do CEG, Lisboa*, p. 15.
- Alcoforado, M.J., Andrade, H., 2006. Nocturnal urban heat island in Lisbon (Portugal): main features and modelling attempts. *Theor. Appl. Climatol.* 84 (1), 151–159. <https://doi.org/10.1007/s00704-005-0152-1>.
- Alcoforado, M.J., Andrade, H., Lopes, A., Vasconcelos, J., 2009. Application of climatic guidelines to urban planning: the example of Lisbon (Portugal). *Landsc. Urban Plan.* 90 (1–2), 56–65. <https://doi.org/10.1016/j.landurbplan.2008.10.006>.
- Alcoforado, M.J., Lopes, A., Alves, E.D.L., Canário, P., 2014. Lisbon heat island statistical study (2004–2012). *Finisterra* 49 (98), 61–80. <https://doi.org/10.18055/Finis6456>.
- Andrade, H.J.N., 2003. *Bioclima Humano e Temperatura Do Ar Em Lisboa*. Ph.D. Thesis. Physical Geography, Faculty of Letters, University of Lisbon, Lisbon, Portugal.
- Arnfield, A.J., 2003. Two decades of urban climate research: a review of turbulence, exchanges of energy and water, and the urban heat island. *Int. J. Climatol. J. R. Meteorol. Soc.* 23 (1), 1–26. <https://doi.org/10.1002/joc.859>.
- Correia, E., 2019. *Mapas Climáticos Urbanos - Geometria e densidade urbana atual. Relatório. In: Cartografia de Vulnerabilidade Térmica – Mapeamento dos efeitos das Ondas de Calor em Lisboa, face às projeções climáticas. Câmara Municipal de Lisboa.*
- Correia, E., 2020. *Mapas Climáticos Urbanos - Geometria e densidade urbana futura. Relatório. In: Cartografia de Vulnerabilidade Térmica – Mapeamento dos efeitos das Ondas de Calor em Lisboa, face às projeções climáticas. Câmara Municipal de Lisboa.*
- De Ridder, K., Lauwaet, D., Maiheu, B., 2015. UrbClim—A fast urban boundary layer climate model. *Urban Clim.* 12, 21–48. <https://doi.org/10.1016/j.uclim.2015.01.001>.
- Du, H., Wang, D., Wang, Y., Zhao, X., Qin, F., Jiang, H., Cai, Y., 2016. Influences of land cover types, meteorological conditions, anthropogenic heat and urban area on surface urban heat island in the Yangtze River Delta urban agglomeration. *Sci. Total Environ.* 571, 461–470. <https://doi.org/10.1016/j.scitotenv.2016.07.012>.
- Giannaros, T.M., Melas, D., 2012. Study of the urban heat island in a coastal Mediterranean City: the case study of Thessaloniki, Greece. *Atmos. Res.* 118, 103–120. <https://doi.org/10.1016/j.atmosres.2012.06.006>.
- He, B.J., 2018. Potentials of meteorological characteristics and synoptic conditions to mitigate urban heat island effects. *Urban Clim.* 24, 26–33. <https://doi.org/10.1016/j.uclim.2018.01.004>.
- Hidalgo, J., Jougla, R., 2018. On the use of local weather types classification to improve climate understanding: an application on the urban climate of Toulouse. *PLoS One* 13 (12), e0208138. <https://doi.org/10.1371/journal.pone.0208138>.
- Hijmans, R., van Etten, J., 2012. raster: geographic analysis and modeling with raster data. In: R package version 2.0-12. <http://CRAN.R-project.org/package=raster>.
- Hooyberghs, H., Berckmans, J., Lefebvre, F., De Ridder, K., 2019. C3S\_422\_Lot2 SIS European health. UrbClim extra documentation 1–18. Available on. <https://c3s.climate.copernicus.eu/cdsapp/#/dataset/sis-urban-climate-cities?tab=form>.
- Kourtidis, K., Georgoulas, A.K., Rapsomanikis, S., Amiridis, V., Keramitsoglou, I., Hooyberghs, H., Melas, D., 2015. A study of the hourly variability of the urban heat island effect in the greater Athens area during summer. *Sci. Total Environ.* 517, 162–177. <https://doi.org/10.1016/j.scitotenv.2015.02.062>.
- Lauwaet, D., De Ridder, K., Saeed, S., Brisson, E., Chatterjee, F., Van Lipzig, N.P.M., Hooyberghs, H., 2016. Assessing the current and future urban heat island of Brussels. *Urban Clim.* 15, 1–15. <https://doi.org/10.1016/j.uclim.2015.11.008>.
- Lee, S.H., Baik, J.J., 2010. Statistical and dynamical characteristics of the urban heat island intensity in Seoul. *Theor. Appl. Climatol.* 100 (1), 227–237. <https://doi.org/10.1007/s00704-009-0247-1>.

- Liu, Y., Li, Q., Yang, L., Mu, K., Zhang, M., Liu, J., 2020. Urban heat island effects of various urban morphologies under regional climate conditions. *Sci. Total Environ.* 743, 140589 <https://doi.org/10.1016/j.scitotenv.2020.140589>.
- Lopes, A., 2003. Modificações no clima de Lisboa como consequência do crescimento urbano. Vento, ilha de calor de superfície e balanço energético. PhD thesis in Physical Geography presented to Faculdade de Letras, Universidade de Lisboa. Universidade de Lisboa, Lisbon, p. 354.
- Lopes, A., Saraiva, J., Alcoforado, M.J., 2011. Urban boundary layer wind speed reduction in summer due to urban growth and environmental consequences in Lisbon. *Environ. Model. Softw.* 26, 241–243. <https://doi.org/10.1016/j.envsoft.2010.05.015>.
- Lopes, A., Alves, E., Alcoforado, M.J., Machete, R., 2013. Lisbon urban heat island updated: new highlights about the relationships between thermal patterns and wind regimes. *Adv. Meteorol.* 2013 <https://doi.org/10.1155/2013/487695>.
- Lopes, A., Fragoso, M., Correia, E., 2018. Contextualização climática (Cap. 3) e Cénarização bioclimática (Cap. 4). In: Plano Metropolitano de Adaptação às Alterações Climáticas, Volume I - Definição do Cenário Base de Adaptação para a AML, pp. 71–168.
- Lopes, A., Oliveira, A., Correia, E., Reis, C., 2020. Identificação das Ilhas de Calor Urbano e Simulação para as Áreas Críticas da Cidade de Lisboa-Fase 1—Caraterização e Cartografia das Ilhas de Calor Atuais. Câmara Municipal de Lisboa, Lisboa, Portugal (in Portuguese).
- Lowry, W.P., 1977. Empirical estimation of urban effects on climate: a problem analysis. *J. Appl. Meteorol. Climatol.* 16 (2), 129–135.
- Martin-Vide, J., Sarricolea, P., Moreno-García, M.C., 2015. On the definition of urban heat island intensity: the “rural” reference. *Front. Earth Sci.* 3, 24. <https://doi.org/10.3389/feart.2015.00024>.
- Morris, C.J.G., Simmonds, I., Plummer, N., 2001. Quantification of the influences of wind and cloud on the nocturnal urban heat island of a large city. *J. Appl. Meteorol. Climatol.* 40 (2), 169–182. [https://doi.org/10.1175/1520-0450\(2001\)040<0169:QOTIOW>2.0.CO;2](https://doi.org/10.1175/1520-0450(2001)040<0169:QOTIOW>2.0.CO;2).
- Ngarambe, J., Oh, J.W., Su, M.A., Santamouris, M., Yun, G.Y., 2021. Influences of wind speed, sky conditions, land use and land cover characteristics on the magnitude of the urban heat island in Seoul: an exploratory analysis. *Sustain. Cities Soc.* 71, 102953 <https://doi.org/10.1016/j.scs.2021.102953>.
- Nogueira, M., Lima, D.C., Soares, P.M., 2020. An integrated approach to project the future urban climate response: changes to Lisbon’s urban heat island and temperature extremes. *Urban Clim.* 34, 100683 <https://doi.org/10.1016/j.uclim.2020.100683>.
- Oke, T.R., Mills, G., Christen, A., Voogt, J.A., 2017. Urban climates. Cambridge University Press. <https://doi.org/10.1017/9781139016476>.
- Oliveira, A., Lopes, A., Niza, S., 2020a. Local climate zones datasets from five southern European cities: Copernicus based classification maps of Athens, Barcelona, Lisbon, Marseille and Naples. Data in brief 31, 105802. <https://doi.org/10.1016/j.dib.2020.105802>.
- Oliveira, A., Lopes, A., Niza, S., 2020b. Local climate zones in five southern European cities: an improved GIS-based classification method based on Copernicus data. *Urban Clim.* 33, 100631 <https://doi.org/10.1016/j.uclim.2020.100631>.
- Oliveira, A., Lopes, A., Correia, E., Niza, S., Soares, A., 2021. Heatwaves and summer urban Heat Islands: a daily cycle approach to unveil the urban thermal signal changes in Lisbon, Portugal. *Atmosphere* 12 (3), 292. <https://doi.org/10.3390/atmos12030292>.
- Peel, M.C., Finlayson, B.L., McMahon, T.A., 2007. Updated world map of the Köppen-Geiger climate classification. *Hydrol. Earth Syst. Sci.* 11 (5), 1633–1644. <https://doi.org/10.5194/hess-11-1633-2007>.
- Pereira, A.R., 2003. Geografia Física e Ambiente-Diversidade do Meio Físico e Recursos Naturais. Atlas da Área Metropolitana de Lisboa 47–65.
- Reis, C., Lopes, A., Correia, E., Fragoso, M., 2020. Local weather types by thermal periods: deepening the knowledge about Lisbon’s urban climate. *Atmosphere* 11 (8), 840. <https://doi.org/10.3390/atmos11080840>.
- United Nations. Department of Economic and Social Affairs, Population Division. Available online. <https://www.un.org/en/development/desa/population/index.asp> (assessed on 23 March 2021).
- Vasconcelos, J., Lopes, A., 2006, June. Recent urban development trends and its implication on the estuarine breezes in Lisbon, Portugal. In: Proceedings of the 6th International Conference on Urban Climate, Vol. 12, p. 16.
- Yang, X., Chen, Y., Peng, L.L., Wang, Q., 2020. Quantitative methods for identifying meteorological conditions conducive to the development of urban heat islands. *Build. Environ.* 178, 106953 <https://doi.org/10.1016/j.buildenv.2020.106953>.
- Zhou, B., Lauwaet, D., Hooyberghs, H., De Ridder, K., Kropp, J.P., Rybski, D., 2016. Assessing seasonality in the surface urban heat island of London. *J. Appl. Meteorol. Climatol.* 55 (3), 493–505. <https://doi.org/10.1175/JAMC-D-15-0041.1>.